Optical Engineering

OpticalEngineering.SPIEDigitalLibrary.org

Optical displacement metrology using alternating direction Moire

Kyoichi Suwa
Koji Kaise
Hiroki Tateno
Nobutaka Magome

SPIE.

Optical Engineering 53(8), 084101 (August 2014)

Optical displacement metrology using alternating direction Moire

Kyoichi Suwa,[a,*] Koji Kaise,[a] Hiroki Tateno,[a] and Nobutaka Magome[b]
[a]Nikon Corporation, Tokyo 100-8331, Japan
[b]Nikon Research Corporation of America, Belmont, California 94002, United States

Abstract. We develop a new double exposure Moire method for an optical registration metrology system in photolithography. Our method enables us to achieve at least a factor of 10 improvements in precise displacement metrology using a conventional optical sensor. We utilize a new registration mark printed to the photoresist on a bare silicon wafer using a double exposure of the gratings. The mark consists of two types of Moire with opposite phases. The two types of Moire are oriented in alternate directions. Displacement is measured from the distance between the positions of the two types of Moire in analogy with the conventional registration method. This concept is called alternating direction Moire. Performance is experimentally confirmed using an i-line wafer exposure apparatus. Precision is improved by up to 32 times as compared with the conventional method and can be applied to other Moire metrologies. © *The Authors. Published by SPIE under a Creative Commons Attribution 3.0 Unported License. Distribution or reproduction of this work in whole or in part requires full attribution of the original publication, including its DOI.* [DOI: 10.1117/1.OE.53.8.084101]

Keywords: semiconductor exposure apparatus; registration metrology; alternating direction Moire; double exposure; bar-in-bar method; differential method; immersion ArF; error reduction.

Paper 140183 received Jan. 31, 2014; revised manuscript received Jun. 25, 2014; accepted for publication Jul. 8, 2014; published online Aug. 5, 2014.

1 Introduction

A wafer aligner is a semiconductor exposure apparatus that aligns a wafer to a mask for each exposure field. Using a stage that sequentially moves field by field, the exposure apparatus can expose a field with a series of alignment sequence steps until the entire wafer surface is exposed. An optical registration metrology system (ORMS) measures the amount of exposure displacement error. Using some form of photolithography registration metrology, ORMS measurements are possible during the alignment process using wafer alignment optics installed in the wafer aligner. Occasionally, these measurements are done with an independent ORMS, which is a commercially available tool. Hereafter, we define ORMS to measure the photoresist marks on bare silicon wafers only. ORMS will then be used mainly for analysis of machine performance, which is very useful for wafer aligners.

The precision of the ORMS sensors has two limitations. The first limitation relates to one-dimensional (1-D) laser spot sensors.[1] When a wafer must be moved beneath a fixed optical sensor,[1] a scanning stage for providing object movement is required for 1-D scanning optical sensors. The error in the position of the laser metrology system for stage monitoring is generally larger than that of the optical sensor due to air temperature fluctuations and high frequency vibrations of machine components,[2] which are beyond the frequency response of laser metrology, so the measurement precision can never be small when using conventional metrological methods. The second limitation occurs when a two-dimensional (2-D) imaging sensor is used to measure a motionless mark.[3] It is difficult to improve the measurement precision in this imaging mode due to the limits associated with the optical image magnification and sensor pixel size reduction. Other types of difficulties also arise when ensuring adequate intensity to the solid state imaging pixels. In the conventional approach, reducing the measurement error involves moving the wafer stage very slowly and taking a large number of data points, N. However, the reducing factor of the error is proportional to $1/\sqrt{N}$, and so an increasing N is time consuming. An alternative approach to overlay measurements employs scatterometry,[4] which is used to reconstruct the three-dimensional (3-D) shape of a registration mark from diffracted light. Although this method has the potential to meet the requirements for registration metrology, lengthy electromagnetic field calculations are required.

In the field of optical measurements, the Moire effect is a well-studied phenomenon.[5,6] The Moire method has a particularly unique advantage in that it can significantly improve the precision with no further demands on the sensitivity of the optical sensor. For this reason, the Moire method is widely used for optical displacement measurements in optical encoders[2,7,8] and curved surface metrology.[9–12] We attempt here to implement Moire technologies into ORMS in order to improve the measurement precision.

There is much previous research in Moire, in particular for measuring 3-D topology. However, in the context of ORMS applications, our implementation to photolithography belongs to 2-D Moire measurements, similar to that found in optical encoders. With regard to an optical encorder, Ref. 8 has proposed an electrical signal process using two independent Moire fringe signals with the same phase. Many types of Moire measurements utilize a 2-D monitor camera to observe a real-time topological deformation.[12,13] Kafri has studied a double exposure technique[5,11] in which the camera film realizes a Moire fringe image by exposing a shifted grating on a previously exposed grating as a reference pattern.

*Address all correspondence to: Kyoichi Suwa, E-mail: kyoichi.Suwa@nikon.com

In registration metrology, measurement of the displacement between two points by photoresist images through double exposure is required. The photoresist image can indicate problems in the exposure of a wafer aligner, such as registration error, machine vibration, and exposure stage error. Such information is valuable because one can perform a calibration for the wafer aligner. The biggest advantage of using Moire technology for ORMS is that the physical quantity to be measured is highly magnified. For a double-exposed wafer, we measure the distance between two sequentially exposed marks. The distance is magnified by the Moire phenomena and calculated by dividing the Moire magnification factor from the measured distance. In this case, theoretically, the measurement error is not magnified. Therefore, the division operation reduces the measurement error with the inverse of the Moire magnification factor. As compared to conventional approaches for reducing the error, our method does not require slow machine movements to record a large number of data points.

In Sec. 2, we describe our derived Moire method, called the alternating direction Moire (ADM). Applications to ORMS measurements are described in Sec. 3. From exposure experiments under i-line illumination, we verify the advantages of the ADM method in Sec. 4. In Sec. 5, future applications to the most advanced immersion ArF tools and the possible merit of ADM are discussed.

2 ADM and ORMS

2.1 *ORMS and Bar-in-Bar Method*

ORMS measurement precision is expressed by $\sigma_{\mathrm{metrology}}$. A first mark or set of marks is created on a wafer by a first exposure. A second mark or set of marks is created by a second exposure. Assume that σ denotes the measurement precision of any one of the photoresist marks obtained with metrology optics. Then, σ is the measurement error of the sensor defined as the statistical error distribution from numerous data points, as described in the Appendix. Assuming that a conventional ORMS measures the distance between two marks, $\sigma_{\mathrm{metrology}}$ is given by

$$\sigma_{\mathrm{metrology}} = \sqrt{2}\sigma. \tag{1}$$

In our case, the marks are photoresist marks so that there is less waveform error for the optical signal.

In conventional systems, the fundamental mark arrangements for ORMS are the box-in-box[14,15] or bar-in-bar.[15] In Fig. 1, the sequential process of the double exposure for the bar-in-bar system is shown. In this process, two types of reticles, $R1$ and $R2$, are used for the photomask. After the reticle $R1$ is exposed on the wafer and the reticle $R2$ is also exposed with the stage in motion to make the bar-in-bar pattern on the photoresist. In the case of the bar-in-bar system, a line is exposed between the two previously exposed lines. The relative position of the center line from the two outside lines corresponds to both the polarity of the direction and the amount of displacement. In this paper, we call this metrology method the differential method. This bar-in-bar system is also known as electrical micromeasurement.[16]

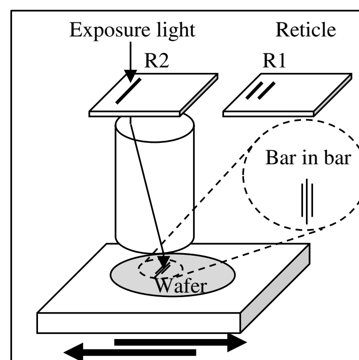

Fig. 1 Double exposure to print bar-in-bar marks on the wafer using reticle 1 and reticle 2.

2.2 *Alternating Direction Moire*

To implement Moire metrology into the bar-in-bar method for ORMS, we develop a new concept using two types of Moire, $+\theta$ and $-\theta$, with opposite phases. Figure 2 shows the schematics of the general principle of ADM where the $-\theta$ Moire is assigned to A and A', and the $+\theta$ Moire is assigned to B. The Moire A and A' correspond to the two outside lines in the bar-in-bar system. Moire B corresponds to the center line of the bar-in-bar system. As in the bar-in-bar system, the offset term is cancelled by the differentiation operation without loss of the precision as

$$\mathrm{ORMS} \equiv [(A - B) - (B - A')]/2. \tag{2}$$

This equation shows the displacement error between gratings $G1$ and $G2$ as shown in Fig. 2.

It is notable that there is a large magnification factor for the ADM in comparison to the bar-in-bar mark, which strongly reduces the measurement errors.

3 Double Exposure ADM Method with Photoresist Mark

3.1 *Basic Concept in Practice*

We propose the ADM method for ORMS. The first and the second exposures are initially performed for two different mask patterns consisting of arrays of lines. Resist development leads to marks on the wafer with positions that are very sensitive to stage alignment errors. Chromium lines on one mask have an inclination angle, θ, with respect to the lines on the other mask. The overlapped areas of the chromium lines of the two masks lead to wedge-shaped unexposed areas on the wafer, which emerge as a positive photoresist pattern after development. The resulting set of unexposed patterns is in the form of a Moire pattern. Assuming the stage moves in the Y-direction in order to overlap the two patterns, the resulting marks are displaced in the X-direction by an amount related to the inclination angle and the displacement. In particular, a change in displacement DY causes a change of $DX = DY(1/\tan\theta)$ in the X-direction. The factor $(1/\tan\theta)$ is referred to as the Moire multiplication ratio.

This procedure is used to measure the distances between adjacent marks and then to divide the measured distances by the Moire multiplication ratio. It should be noted that all measurement errors are reduced by a factor of the Moire

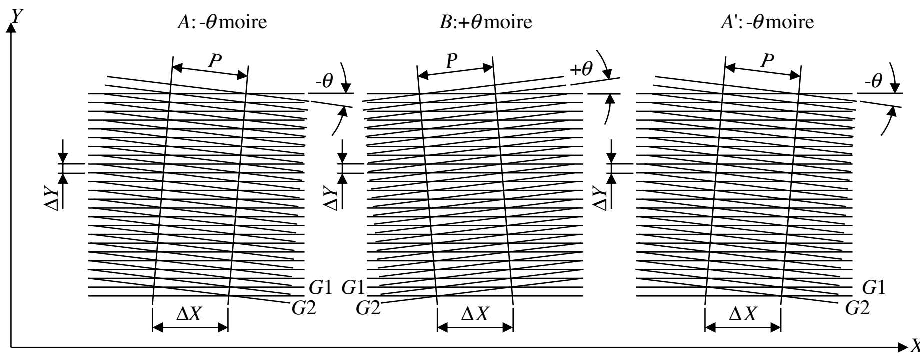

Fig. 2 General principle of alternating direction Moire (ADM); the notation is different from that of chapter 3. The Moire pattern *A* observed when two grating images *G*1 and *G*2 are tilted with an angle $-\theta$; if the grating *G*1 is moved a distance Δy in the *y*-direction, the Moire pattern will move a distance $\Delta X = -\Delta Y / \tan\theta$ in the *x*-direction. The Moire pattern B tilted with an angle $+\theta$; if the grating *G*1 is moved a distance Δy in the *y*-direction, the Moire pattern will move a distance $\Delta X = \Delta Y / \tan\theta$ in the *x*-direction. Pattern *A* and pattern *B* have opposite phase. Pattern A' is identical to pattern *A*, but the position is the opposite of pattern *A*.

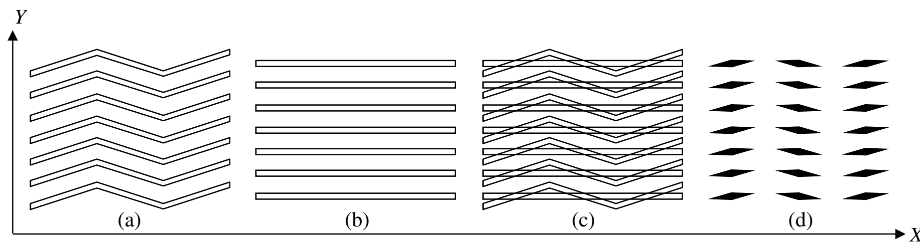

Fig. 3 Combination of Moire photoresist patterns. (a) The first mask pattern. (b) The second mask pattern. (c) Double exposed image. (d) Patterns after development used for ADM. There are seven pairs of zigzag and straight lines.

multiplication ratio. In creating Moire photoresist images, the marks should meet the requirements for the ADM method, a zero point of the position should exist, and the amount of its shift from the zero point should include directional information concerning the positional error.

Figure 3 shows how Moire photoresist images are created with the double exposure process. A *Y*-direction shift of the wafer, Δ, causes an *X*-direction shift of the mark, Λ. The shift Δ is multiplied by the ratio, $1/\tan\theta$, to create the latter shift through the double exposure of a zigzag mark and a straight line mark. θ is an angle between the zigzag and straight lines. At least three points of Moire photoresist images are needed to meet the requirements for the ADM method. The changes in the coordinates of $X1$ to $X2$ and that of $X2$ to $X3$ are related to alignment errors through the Moire effect. Figure 4 shows the Moire photoresist images when Δ is zero. The zigzag line in this figure is the centerline of the zigzag pattern of the second mask pattern. The finite Δ case is shown in Fig. 5.

3.2 *Error Analysis of Measurements*

We discuss the estimation of ADM measurement errors, where the following analysis is applicable to any type of ORMS sensor. We analyze the ADM measurement error in ORMS, assuming measurement error follows a normalized Gaussian distribution, hereafter called the normal distribution in this paper, without loss of generality. The measurement error is reduced by a factor equal to the inverse Moire multiplication ratio. The coordinates of three Moire photoresist marks are given by

$$X1 = -L + \Lambda + \varepsilon_1, \tag{3}$$

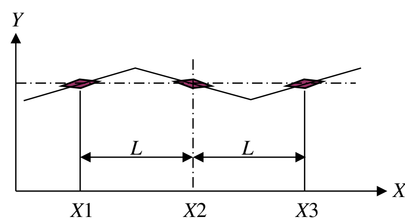

Fig. 4 Example of double exposed patterns. Dot-dashed line represents the case where the *Y*-direction shift Δ is zero.

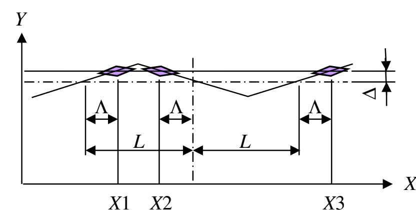

Fig. 5 Solid line represents the case where the *Y*-direction shift is Δ. *X*1, *X*2, and *X*3 are the coordinates of the marks shifted by the multiplied shift, Λ.

$$X2 = -\Lambda + \varepsilon_2, \tag{4}$$

$$X3 = L + \Lambda + \varepsilon_3, \tag{5}$$

$$\Lambda = \Delta(1/\tan\theta). \tag{6}$$

The measurement error of the detection for each mark is written as ε_i. The physical quantity measured in this method $\Lambda_{\text{measured}}$ is defined as the difference between the distance of $X1$ and $X2$ and that of $X2$ and $X3$, as depicted in Figs. 4 and 5.

$\Lambda_{\text{measured}}$ can be expressed in terms of the true value Λ.

$$\Lambda_{\text{measured}} = [(X3 - X2)/2 - (X2 - X1)/2]/2 = \Lambda + [(\varepsilon_1 + \varepsilon_3 - 2\varepsilon_2)/2]/2. \tag{7}$$

Using Eqs. (6) and (7), Δ can be rewritten as

$$\Delta_{\text{measured}} = \tan\theta[(X3 - X2)/4 - (X2 - X1)/4] = \Delta + \tan\theta(\varepsilon_1 + \varepsilon_3 - 2\varepsilon_2)/4 \tag{8}$$

$$\equiv \Delta + \varepsilon. \tag{9}$$

Finally, Δ_{measured} is defined from $\Lambda_{\text{measured}}$ and ε is the total measurement error.

The measurement error of each mark ε_i is assumed to have a constant variance regardless of θ, although the shape of the Moire photoresist mark appears different depending on the angle. This assumption is discussed in Sec. 5.1 in detail. In order to discuss the θ dependence of ε, we introduce

$$\varepsilon = (\tan\theta/4)\rho. \tag{10}$$

We can show that

$$\rho \sim N(0{,}6\sigma^2), \tag{11}$$

for which the derivation is given in the Appendix.

Referring to Eqs. (11) and (10), ε is expressed as

$$\varepsilon \sim N[0, (\tan\theta/4)^2 \cdot 6\sigma^2]. \tag{12}$$

From Eq. (12), the ORMS precision $\sigma_{\text{metrology}}$ of ADM is

$$\sigma_{\text{metrology}} = \sqrt{(\tan\theta/4)^2 \cdot 6\sigma^2}. \tag{13}$$

Equation (13) indicates that the measurement precision is enhanced in inverse proportion to the Moire multiplication ratio. From the relationship between the X-direction coordinates and the angle θ, the following relation is satisfied: $\Delta_{\text{measured}} \equiv 1/K[(X3 - X2) - (X2 - X1)]$. The factor K is defined as

$$K = 4/\tan\theta. \tag{14}$$

The Moire sensitivity and reduction ratio of the error can be adjusted by the appropriate selection of θ. K is proportional to the Moire multiplication ratio.

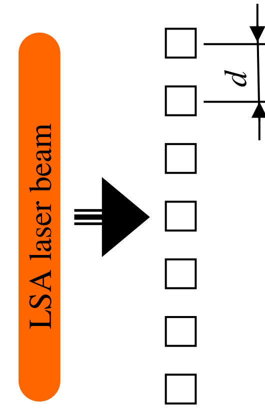

Fig. 6 Laser beam shaped into an elliptic spot. The short axis is about 4-μm long with a 40-μm long axis. Seven marks make up a row with a pitch of $d = 4$ μm.

4 Experimental Results

4.1 *Laser Step Alignment*

We focus our attention on wafer alignment optics that use a laser spot.[1] Under this assumption, the laser spot can produce a significant amount of scattered light even for small wedge shapes in Moire photoresist images. Experiments are performed to validate the ADM precision of the 1-D alignment optics equipped with an exposure apparatus and a laser step alignment (LSA) measurement system installed in a Nikon NSR-1755iA (NA = 0.50, illumination NA = 0.30), which is an i-line exposure apparatus. A normally incident laser sheet beam creates an oblong spot on the wafer. As shown in Fig. 6, a periodic array of die-shaped marks is situated on the wafer. When the laser spot is positioned on the marks during the stage scan, the laser beam is diffracted by the marks and detected by an optical device located at an angle $\phi = \sin^{-1}(\lambda/d)$ relative to the wafer surface. The angle is determined by the period of the marks and the wavelength of the laser light.

4.2 *LSA for ADM Measurement*

In Fig. 7, the ADM mark arrangement is displayed as three columns of marks along the X-axis in seven rows with a $d =$ 4 μm pitch. The LSA diffraction signal along the X-axis is shown in Fig. 8. In the process of the stage scans, the light signal consists mostly of light diffracted by the columns of marks.[1,17,18] In the discussion below, the ORMS precision σ is multiplied by a factor of three. In the 3σ expression, all measured values lie within 3 sigma of the mean, or

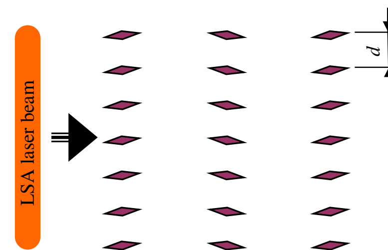

Fig. 7 ADM patterns and one-dimensional laser scanning system (LSA). There are three rows of seven wedge-shaped patterns along the X-direction with a pitch of 4 μm.

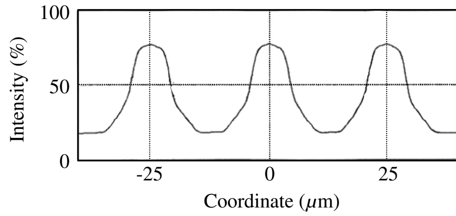

Fig. 8 Waveform of LSA signals.

approximately 99.7%. Note that in Sec. 3, the ORMS precision for ADM is calculated for 1σ.

4.3 *ADM Magnification and Precision Improvement*

We experimentally investigate the validity of ADM by demonstrating that precision improves in inverse proportion to the increasing magnification factor. Masks with several different angles are prepared for the experiment. In Fig. 9, there are two masks with 2-μm line width periodic gratings for the double exposures. The masks are designed to have four different values of K: 10, 16, 20, and 32, corresponding to four different θ of 21.8, 14, 11.3, and 7.1 deg, respectively. As an example, in Table 1, a 2-D of the largest and smallest angle patterns (labeled as $10x$ and $32x$, respectively) are shown. Regarding $K = 1$, we adapt the conventional ORMS experimental data with the arrangement shown in Fig. 6. The ORMS data for $K = 1$ gives a 3σ precision of

$$3\sigma_{\text{i-line,Metrology}} = 14 \text{ nm}. \tag{15}$$

$\sigma_{\text{i-line,Metrology}}$ denotes the precision for an i-line exposure tool and ORMS metrology.

Four different magnification data points for ORMS of ADM are repeatedly taken. From this data, the measurement precision is shown as five dots in Fig. 10, where the vertical and the horizontal axes are expressed on a logarithmic scale. According to the theory of the ADM method, the precision in the experimental data in Fig. 10 has a slope of -1 with respect to magnification. The data fit well to a linear model, with a coefficient of determination R^2 of over 0.93 for five data points, indicating good agreement with the data.

The increased multiplication of ADM in our experiments is consistent with the theoretical prediction calculated according to Eq. (14). At $32x$ ($\theta = 7.1$ deg), the 3σ precision of ORMS using ADM for an i-line exposure apparatus is derived from the linear curve in Fig. 10 as

$$3\sigma_{\text{i-line,Moiremetrology}} = 0.50 \text{ nm}. \tag{16}$$

$3\sigma_{\text{i-line,Moiremetrology}}$ refers to the precision of an i-line tool and ORMS using ADM metrology.

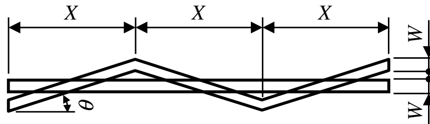

Fig. 9 Design details of ADM patterns.

Table 1 Design rules for 10× and 32× ADM marks in experiments.

Magnification	10×	32×
Length (X)	25 μm	50 μm
Cross angle (θ)	21.8 deg	7.1 deg
Line width (W)	2 μm	2 μm
Range (Y)	±3 μm	±1.1 μm

5 Discussion

5.1 *Verification of Assumptions*

Based on the experimental results shown in Fig. 10, the errors ε_i in Eqs. (3)–(5) reach a constant value. Thus, the assumption in Sec. 3.2, namely that the error expressed by a normal distribution is not influenced by the shape of the mark, is valid under experimental conditions. The LSA system has a constant measurement error, despite the fact that the wedge-shaped mark becomes narrower with an increase in magnification factor K, at least up to $K = 32$.

5.2 *Mask Error Robustness of ADM*

Mask manufacturing errors, including angle error and line roughness error, are discussed in this section. In Fig. 3, given three overlapping exposure points with different line segment angles α, β, and γ, the magnification factor K can be derived from Eqs. (3) to (6) as

$$K = (1/\tan\alpha + 2/\tan\beta + 1/\tan\gamma)/4. \tag{17}$$

Note that when $\alpha = \beta = \gamma = \theta$, Eq. (17) reduces to Eq. (14). In Eq. (17), there is no functional change for ADM excluding the Moire magnification factor K. We can correct the numerical value of K in advance of angle measurements. Under practical conditions, nearly all masks are fabricated from lithography tools using a raster scan method rather than a vector scan. Raster scans have no inherent angle errors, so mask error predominantly originates from random line roughness errors. Consequently, angle errors are of little concern for raster scan-based masks.

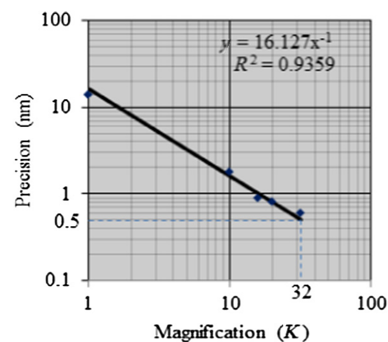

Fig. 10 Relationship between the precision and the magnification, K. The vertical axis shows the optical registration metrology system 3σ precision. The horizontal axis shows ADM magnification K. Five data points for different K values are plotted. The solid line corresponds to a x^{-1} dependence.

5.3 *Future Precision Improvement*

The ADM method is a new methodology that combines the Moire principle with a conventional sensor to detect a resist wedge mark. This method would be relevant to an advanced generation immersion ArF exposure apparatus if mark edge measurements employ a nonstage-scanning sensor, such as a 2-D CMOS image sensor. This assumes that equally precise measurements are possible for CMOS image sensors in comparison to 1-D laser spot sensors.

For a typical immersion ArF exposure apparatus with a 2-D CMOS alignment sensor, the 3σ sensor precision is usually assumed as $3\sigma_{\mathrm{ArF,CMOS}} = 0.5$ nm,[19] where $\sigma_{\mathrm{ArF,CMOS}}$ is the sensor precision of the ArF tool with the 2-D CMOS sensor. Then, from Eq. (1)

$$3\sigma_{\mathrm{ArF,metrology}} = \sqrt{2} \cdot 3\sigma_{\mathrm{ArF,CMOS}} = 0.707 \text{ nm}, \tag{18}$$

where $3\sigma_{\mathrm{ArF,metrology}}$ denotes the ORMS precision of the ArF tool.

The estimated ORMS precision of a 32× angle pattern using ADM for an exposure ArF tool is calculated from Eqs. (15), (16), and (18) as

$$\begin{aligned} &3\sigma_{\mathrm{ArF,Moiremetrology}} \\ &\quad = (3\sigma_{\mathrm{i\text{-}line,Moiremetrology}})(3\sigma_{\mathrm{ArF,metrology}})/(3\sigma_{\mathrm{i\text{-}line,Metrology}}) \\ &\quad = 0.025 \text{ nm}. \end{aligned} \tag{19}$$

Here, $\sigma_{\mathrm{ArF,Moiremetrology}}$ is the ADM precision of the ORMS for the ArF exposure apparatus. This precision is less than 0.1 nm, the desired target number[20] given present semiconductor manufacturing processes. Furthermore, by selecting an appropriate θ, the sensitivity, K, can be adjusted to provide further improvement if needed. It is notable that the ADM technology can offer a new possibility for “picometer” order optical registration metrology.

5.4 *Positive and Negative Resist*

ADM can be applied using either a positive or negative resist. However, the single exposure dose energy for a double exposure is different for positive and negative resists. For a positive resist, E_{p} is greater than E_{t}, where E_{p} is the single dose energy for a positive resist image and E_{t} is the threshold energy above which the positive resist disappears or the negative resist remains after development. For negative resists, E_{n} is less than E_{t}, but $2E_{\mathrm{n}}$ is greater than E_{t}, where E_{n} is the single dose energy for the negative resist image.

5.5 *Nonphotoresist Application*

Our experiment for the ADM is performed in the case of photolithography where the Moire pattern is printed on the photoresist. However, the concept of ADM is general because it is fundamentally derived from the bar-in-bar method. Therefore, beyond the case of photolithography, our ADM pattern is one of the candidates for Moire position measuring metrology for wide areas.

To obtain the ADM marks, we require two sequential exposures, $G1$ and $G2$, in Fig. 2. Thus, it is impossible for ADM to be applied to real-time Moire measurements. If the pattern $G1$ has already been exposed on the wafer plane and the $G2$ reticle is fixed, real-time measurements are possible using a camera. This mode of ADM is not applicable for registration metrology.

6 Conclusions

We developed a new concept for ORMS measurements called the ADM method, which utilizes the double exposure photoresist marks with opposite phases to create a Moire pattern. This measurement method greatly improves precision in inverse proportion to the Moire multiplication ratio. Experiments showed a 0.50 nm (3σ) precision using the optical alignment sensor of an i-line exposure apparatus, a precision 32 times higher than conventional methods. Given an alignment sensor sensitivity adequate for wedge detection using ADM, this method can be applied to the most advanced immersion ArF scanners, with a possible 25 pm (3σ) precision. As compared to the conventional approach to reduce error, our method does not require a large number of slow machine movements because the error is reduced in inverse proportion to the Moire magnification. The concept of ADM is not limited to ORMS and can be applied to other Moire metrologies.

Appendix: ε_i and Summation of σ

The notation ε_i denotes an amount of error in the ORMS measurement in mark detection i, subject to a normal distribution $N(\mu, \sigma^2)$, with mean μ and variance σ^2. We define the expression

$$\varepsilon_i \sim N(\mu, \sigma^2). \tag{20}$$

Since the mean value of the measurement error in this paper is generally zero, ε_i can be expressed as

$$\varepsilon_i \sim N(0, \sigma^2). \tag{21}$$

With respect to ε, the calculation of a unified variance for three marks can be defined as follows. Define ρ as the error associated with three marks combined

$$\rho = \varepsilon_1 + \varepsilon_3 - 2\varepsilon_2. \tag{22}$$

Here, ρ is the random variable and is the equation represented as Eq. (22). It can be represented as

$$\rho \sim N(0, \sigma_{\mathrm{p}}^2), \tag{23}$$

where σ_{p}^2 is the variance of three point measurements. Since $\{\varepsilon_i\}$ can be represented by a uniform value subject to a normal distribution, the unified variance can be calculated as

$$\sigma_{\mathrm{p}}^2 = (1^2 + 1^2 + 2^2)\sigma^2 = 6\sigma^2. \tag{24}$$

Upon substitution of Eq. (24) into Eq. (23), we have Eq. (11).

Acknowledgments

The authors thank Dr. Michael Sogard, Mr. Koichi Matsumoto, Dr. Shinichi Nakajima, Dr. Kazuya Okamoto, and Dr. Tomoya Noda for their valuable suggestions.

References

1. S. Murakami et al., "Laser step alignment for wafer stepper," *Proc. SPIE* **538**, 9–16 (1985).
2. A. H. Slocum, *Precision Machine Design*, Society of Manufacturing Engineers, Dearborn, Michigan (1992).
3. K. Ota, N. Magome, and K. Nishi, "New alignment sensor for wafer stepper," *Proc. SPIE* **1463**, 304–314 (1991).
4. J. Maas et al., "Yield star: a new metrology platform for advanced lithography control," *Proc. SPIE* **7985**, 79850H (2011).
5. O. Kafri and I. Glatt, *The Physics of Moire Metrology*, Wiley, New York (1989).
6. R. F. Anastasi, *An Introduction to Moire Methods With Applications in Composite Materials*, No. MTL TR 92-55, Army Lab Command, Material Technology Lab, Watertown, Massachusetts (1992).
7. R. Chang et al., "Analysis of CCD Moire pattern for micro-range measurements using the Wavelet transform," *Opt. Laser Technol.* **35**(1), 43–47 (2003).
8. J. Liu et al., "Precision position control systems using Moire signals," in *Proc. of the 1995 IEEE IECON 21st Int. Conf. on Industrial Electronics, Control, and Instrumentation, 1995*, Vol. 2, pp. 968–972, IEEE (1995).
9. B. Han, "Thermal stresses in microelectronics subassemblies: quantitative characterization using photo-mechanics methods," *J. Therm. Stresses* **26**(6), 583–613 (2003).
10. S. Yokozeki and T. Suzuki, "Interpretation of the Moiré method for obtaining contours of equal slope from an interferogram," *Appl. Opt.* **9**(12), 2804–2805 (1970).
11. A. Livnat and O. Kafri, "Finite fringe shadow Moire slope mapping of diffusive objects," *Appl. Opt.* **22**(20), 3232–3235 (1983).
12. J. Dhanotia et al., "Slope measurement of bent plates using double grating shearing interferometry," *Appl. Opt.* **50**(18), 2958–2963 (2011).
13. M. Seib and H. Hoefler, "3-D Moire contouring with modified CCD-camera," *Proc. SPIE* **1375**, 28–38 (1989).
14. Y. Cheng et al., "Reduction of image-based ADI-to-AEI overlay inconsistency with improved algorithm," *Proc. SPIE* **8681**, 86812P (2013).
15. M. Adel et al., "Optimized overlay metrology marks: theory and experiment," *Semicond. Manuf.* **17**(2), 166–179 (2004).
16. L. Nugent-Glandorf and T. T. Perkins, "Measuring 0.1-nm motion in 1 ms in an optical microscope with differential back-focal-plane detection," *Opt. Lett.* **29**(22), 2611–2613 (2004).
17. K. Suwa et al., "Automatic laser scanning focus detection method using printed focus pattern," *Proc. SPIE* **2440**, 712–720 (1995).
18. I. Grodnensky et al., "Technique for optical characterization of exposure tool imaging performance down to 100 nm," *J. Vac. Sci. Technol. B* **17**(6), 3285–3290 (1999).
19. Y. Shirata et al., "High-productivity immersion scanner enabling 1× nm hp manufacturing," *Proc. SPIE* **8683**, 86831K (2013).
20. W. H. Arnold, "Metrology in times of shrinking budgets," *Proc. SPIE* **8681**, 868102 (2013).

Kyoichi Suwa received an MS degree from Osaka University in 1973, and participated in the development of the wafer aligner, macroinspection, and the LCD aligner. He was a previous member of the Nikon board of directors. His most recent published paper appeared in *Applied Optics*.

Koji Kaise has worked for Nikon since 1980 as a senior development engineer.

Hiroki Tateno received a BSc degree from Meiji University in 1981. He has been working on the development of optical metrology.

Nobutaka Magome received an MS degree from Tokyo T. Tech. in 1980. He has been a principal optical researcher. He is now a Nikon fellow.